

Alternative Modes of Tyrosyl Phosphopeptide Binding to a Src Family SH2 Domain: Implications for Regulation of Tyrosine Kinase Activity[†]

John E. Ladbury,^{*,‡,§} Meike Hensmann,[‡] George Panayotou,^{||} and Iain D. Campbell[‡]

Oxford Centre for Molecular Sciences, University of Oxford, South Parks Road, Oxford OX1 3QT, U.K., and Ludwig Institute for Cancer Research, University College London, Middlesex Hospital Branch, 91 Riding House Street, London W1P 8BT, U.K.

Received March 5, 1996; Revised Manuscript Received April 25, 1996[®]

ABSTRACT: Src homology 2 (SH2) domains interact with proteins containing phosphorylated tyrosine residues and as such play a key role in mediating tyrosine kinase signal transduction. Determination of how these interactions maintain specificity is central to understanding the mechanism of this intracellular signal processing. In the Src family tyrosine kinases specificity is enhanced by a form of regulation based on binding of a phosphotyrosine, pY, and its proximal amino acid sequence from the C-terminus to the SH2 domain of the same protein (autoregulation) or to a similar protein (homodimeric regulation). Activation of the protein is accomplished by removal of this regulatory interaction by competition from a "specific" interacting ligand. We adopt the SH2 domain from a member of the Src family, Fyn (whose predominant physiological role is in initiation of signals from the T-cell receptor complex), to explore the differences in structural, thermodynamic, and kinetic determinants of regulatory and specific interactions using tyrosyl phosphopeptides based on the C-terminus and on a putative physiological interacting species from the hamster middle-sized tumor antigen. The specific peptide interacts with micromolar affinity via embedding the pY and an isoleucine residue (in the pY + 3 position) in two deep pockets. This leads to a large favorable enthalpic contribution to free energy. The regulatory peptide interacts in the pY pocket which forms a pivot for the rest of the molecule which is dynamic. These structural data for the regulatory peptide are supported by the observation of a more favorable entropic term and a complex mode of binding revealed by kinetic analysis.

Src homology 2 (SH2) domain interactions with proteins containing phosphorylated tyrosine (pY)¹ residues play a crucial role in numerous cytoplasmic signal transduction pathways (Pawson & Schlessinger, 1993; Schlessinger, 1994; Pawson, 1994). For the integrity of a signal passing from the cell membrane receptor to the nucleus, it is important that these interactions remain mutually exclusive. Understanding how SH2 domains maintain their specificity for a given pY-containing peptide is important in interpreting the mechanisms involved in tyrosine kinase signaling and in attempting to influence these by pharmaceutical intervention.

An additional form of control is exerted in interactions of the SH2 domain of Src family tyrosine kinases. Nine proteins have so far been identified as members of the Src family. These all comprise a modular structure with a unique N-terminal sequence, myristylated for tethering to the cytoplasmic side of the membrane, an SH3 domain, the SH2

domain, and a kinase domain. The SH2 domains of the Src family have high sequence and structural similarity (Waksman et al., 1992; Eck et al., 1993; Kuriyan & Cowburn, 1993). An essential feature of Src family SH2 domain function is regulation of enzyme activity. Current models for this indicate that this is centered around a tyrosine residue in the C-terminal end of the protein (Cantley et al., 1991). When this residue is phosphorylated, it is proposed to bind either to the intramolecular SH2 domain (autoregulation) or to the SH2 domain of a proximal molecule forming a homodimeric species. Both conformations would lead to a low activity state. *In vivo* activation of the enzyme is likely to involve the displacement by other phosphotyrosine-containing ligands. This model is supported by the observation that mutations of the tail region result in a constitutively active enzyme and cell transformation [e.g., Cooper and Rothwell (1993)].

In vitro studies on the specificity of SH2 domains for short pY-containing peptides indicate that Src family SH2 domains have highest affinity for the residues EEI C-terminal to the pY (Songyang et al., 1993; Songyang & Cantley, 1995). This corresponds to the motif found in the hamster middle-sized tumor (HmT) antigen which is known to bind and activate Src family members *in vivo* (Courtneidge et al., 1991) and thus represents a "specific" interaction. Structural studies indicate that these peptides bind in an extended conformation by embedding the pY and the isoleucine (in the pY + 3 position) in two pockets on the protein surface (Waksman et al., 1993; Eck et al., 1993; Mikol et al., 1995). The phosphate group of the pY is stabilized in its pocket by a network of hydrogen bonds which include a bidentate salt

[†] We thank the Wellcome Trust for support to M.H. and I.D.C. J.E.L. is a Wellcome Trust Research Career Development Fellow. G.P. is supported by the Ludwig Institute. OCMS is funded by BBSRC, MRC, and EPSRC.

* Address correspondence to this author.

[‡] Oxford Centre for Molecular Sciences, University of Oxford.

[§] Current address: Department of Biochemistry, University College London, 91 Riding House St., London W1P 8BT, U.K.

^{||} Ludwig Institute for Cancer Research, University College London.

[®] Abstract published in *Advance ACS Abstracts*, August 1, 1996.

¹ Abbreviations: SH, Src homology; NOE, nuclear Overhauser effect; pYHmT, tyrosyl phosphopeptide based on hamster middle-sized tumor antigen; pY, tyrosyl phosphopeptide; pY531, tyrosyl phosphopeptide based on the region proximal to tyrosine in position 531 on Fyn; DTT, 1,4-dithio-DL-threitol; KP_i, potassium phosphate; NMR, nuclear magnetic resonance; ITC, isothermal titration calorimetry; DSC, differential scanning calorimetry; SPR, surface plasmon resonance.

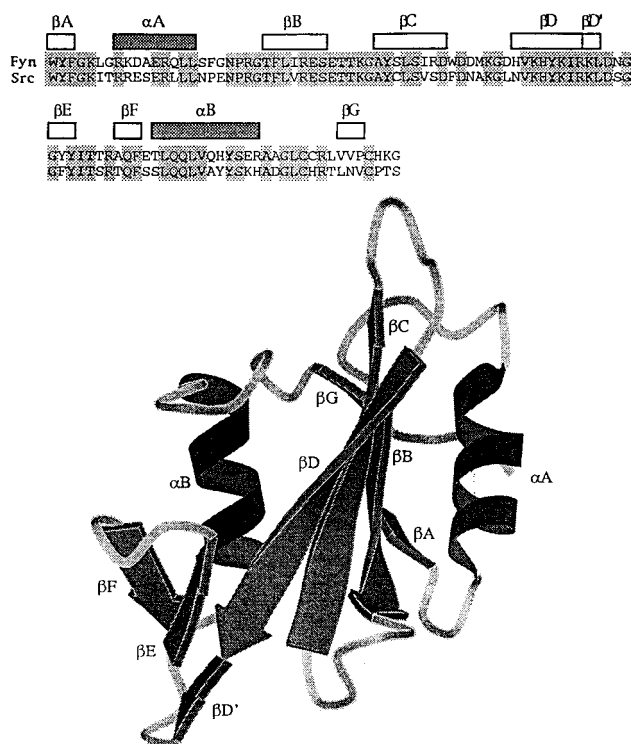


FIGURE 1: (Top) Primary sequence alignment of the SH2 domains of Fyn and Src demonstrating regions of high sequence homology (gray shading) and the location of secondary structural elements. (Bottom) Backbone MOLSCRIPT (Kraulis, 1991) diagram of a model of the Fyn SH2 structure based on the crystal structure of the SH2 domain of Src (Waksman et al., 1992), using the labeling scheme of Eck et al. (1992).

bridge. In the regulatory peptide the amino acids proximal to the pY do not have the EEI motif; instead, a glycine residue is found in the pY + 3 position. The equilibrium dissociation constants (K_D) have been determined for the interaction of the Src and Lck SH2 domains with peptides corresponding to regions around both the regulatory and HmTpY residues (Payne et al., 1993; Lemmon & Ladbury, 1994). The affinity of a regulatory peptide was shown, in these cases, to be approximately 1 order of magnitude lower than a specific peptide at pH 6.8 and 25 °C (Ladbury et al., 1995).

In this investigation we address the question of what are the differences in the structural, thermodynamic, and kinetic determinants of binding for regulatory and specific interactions with Src family SH2 domains? Here we have adopted a model SH2 domain, that of the Src-related tyrosine kinase p59^{fyn}, or Fyn. Although there is no reported solution or crystal structure of the Fyn SH2 domain, the structure can be assumed to be similar to the structure of known Src-related SH2 domains (Waksman et al., 1992, 1993; Eck et al., 1993); there is 65% amino acid sequence identity, particularly in regions of secondary structure (Figure 1), and NMR data confirm that the locations of the secondary structure of the Fyn SH2 domain are in the same positions as in Src (unpublished data). Nuclear magnetic resonance (NMR) is used here to determine and compare the binding surfaces that interact with representative regulatory and specific phosphopeptides. Line-shape analysis is also used to explore the kinetics and mechanism of the binding process in each case. Using this information together with thermodynamic

and kinetic data, gathered from isothermal titration calorimetry (ITC) and surface plasmon resonance (SPR) studies, detailed comparisons of the different binding can be made.

EXPERIMENTAL PROCEDURES

Protein Expression and Purification. The SH2 domain studied corresponds to amino acids 139–255 of human c-Fyn (Semba et al., 1986). It was expressed in *Escherichia coli* BL21 cells as a glutathione *S*-transferase (GST) fusion (the plasmid was a kind gift from S. Courtneidge). Affinity-purified fusion protein was cleaved with human thrombin (Sigma) and the free SH2 domain separated in one step using size exclusion chromatography (Pharmacia S-100 HR, i.d. 2.6 cm). For all experiments the protein was exchanged from the purification buffer (50 mM Tris, 150 mM NaCl, 5 mM DTT, pH 8.0) into low-salt phosphate buffer (10 mM KPi, 30 mM NaCl, 5 mM DTT, pH 6.0). The protein concentration was determined using an extinction coefficient at 280 nm of 19.24 mM⁻¹·cm⁻¹.

Tyrosyl Phosphopeptide Synthesis. Peptides were prepared using 9-fluoromethoxycarbonyl (Fmoc) chemistry, incorporating phosphotyrosine in the synthesis (Piccione et al., 1993; Kitas et al., 1993). The sequences of the peptides were as follows: regulatory pY531 (Fyn C-terminal), ATEPQ(pY)-QPGEN; specific pYHmT, EPQ(pY)EEIPIYL. The peptides were purified as previously described (Hensmann et al., 1994; Ladbury et al., 1995). Peptide concentrations were determined by mass and verified by amino acid analysis and mass spectrometry.

Isothermal Titration Calorimetry (ITC). Isothermal titration calorimetry (ITC) provides an accurate method for the direct determination of the binding constant, K_B , and the enthalpy, ΔH , for the equilibrium process of going from the free to bound state from direct measurement of the heat of interaction over a series of injections of one interactant into the other. These data provide a full thermodynamic characterization of the interaction since

$$-RT \ln K_B = \Delta H - T\Delta S^\circ = \Delta G^\circ$$

where R is the gas constant, T is the absolute temperature, $K_B = 1/K_D$, ΔS° is the entropy of the interaction, and ΔG° is the free energy for the interaction (Wiseman et al., 1989). Experiments were performed as previously described by Lemmon and Ladbury (1994) and Ladbury et al. (1995) using a MCS calorimeter (MicroCal Inc., Northampton, MA); the data were fit with least squares regression using ORIGIN software. The SH2 polypeptide and the tyrosyl phosphopeptide were dissolved in 10 mM KPi, 30 mM NaCl, and 5 mM DTT, pH 6.0, and titrations were done at 30 °C. The heats of dilution obtained from separate titrations of peptide into buffer and buffer into SH2 polypeptide were subtracted from the raw data for the peptide–SH2 titration prior to data analysis. The data reported in Table 1 are average values for at least two independent titrations at each temperature.

Surface Plasmon Resonance (SPR). Determination of the equilibrium constants of the SH2–pY peptide interactions was done as described by Panayotou et al. (1993) and Ladbury et al. (1995). Peptides were biotinylated, separated by reversed-phase HPLC, and analyzed by mass spectrometry. Peptides with a single biotin molecule at their N-terminus were captured on avidin immobilized on the

Table 1: Thermodynamic Parameters Determined for the Binding of SH2 Domains to Tyrosylphosphopeptides at pH 6.0^a

temp (°C)	stoichiometry	$K_B \times 10^{-6} (M^{-1})$	$K_D (\mu M)$	$\Delta G^\circ (kJ \cdot mol^{-1})$	$\Delta H (kJ \cdot mol^{-1})$	$\Delta S^\circ (J \cdot mol^{-1} \cdot K^{-1})$
Specific Peptide pYHmT						
25	1.02 (± 0.02)	1.36 (± 0.02)	0.74	-35.0	-36.6 (± 0.4)	-5.4
30	1.00 (± 0.03)	0.70 (± 0.07)	1.43	-33.9	-42.2 (± 0.1)	-27.4
Regulatory Peptide pY531						
25	1.01 (± 0.02)	0.04 (± 0.01)	24.39	-26.3	-18.1 (± 0.2)	+27.5
30	1.00 (± 0.03)	0.02 (± 0.01)	47.84	-25.1	-20.2 (± 0.4)	+16.2

^a Errors in parentheses correspond to those obtained from fits of ITC data; see Experimental Procedures.

Dextran-coated surface of the sensor chip. Proteins were transferred into running buffer (20 mM HEPES, pH 7.4, 150 mM NaCl, 4 mM DTT, 0.005% Tween 20) and passed over the peptides at a constant flow rate of $5 \mu L \cdot min^{-1}$ at 25 °C. A separate surface, coated with a nonphosphorylated peptide, was used as a control, and the response obtained at different protein concentrations was subtracted from that of the phosphorylated peptides in order to correct for "bulk" effects of the injected protein. The response obtained at equilibrium was plotted versus the protein concentration injected, and Scatchard plots were used to calculate the binding constants. The Fyn-SH2 interactions with the peptides were also analyzed from the sensorgrams obtained, in terms of on and off rates (k_{on} and k_{off} , respectively), thus giving an independent determination of the binding constant from $K_B = k_{on}/k_{off}$.

Nuclear Magnetic Resonance (NMR). The samples for NMR spectroscopy were prepared by concentrating uniformly ^{15}N -labeled protein after buffer exchange to a final concentration of 1–1.5 mM. D_2O was added at 5% (v/v). Samples of peptide for the titration studies were prepared by lyophilizing aliquots of an aqueous peptide solution of known concentration. Experiments were performed on an in-house-designed spectrometer operating at a 1H frequency of 500 MHz. All spectra were recorded at 30 °C using trim pulses for solvent signal suppression and GARP-1 phase modulation for ^{15}N decoupling during acquisition (Shaka et al., 1985). Sign discrimination in t_1 was achieved using the States time-proportional phase incrementation method (Marion et al., 1989). Two-dimensional $\{^1H-^{15}N\}$ 1H -detected single-quantum heteronuclear chemical shift correlation spectra were acquired with 2048 t_2 data points, 256 t_1 increments, and spectral widths of 8000 Hz (1H) and 2600 Hz (^{15}N), respectively. All data were processed on SUN workstations using the FELIX 2.3 software package (Hare Research, Inc.). Skewed and phase-shifted sine-bell weighting functions as well as zero filling were applied before Fourier transformation.

NMR Line-Shape Analysis. The simulations of the NMR line shapes have been previously described (Hensmann et al., 1994). The simulations used either a two- or three-site exchange model as indicated in Figure 4. Chemical shifts, transverse relaxation rates, and individual rate constants were input for each species. The solutions were used to simulate free induction decays, which were processed in the same way as the experimental data to allow direct comparison.

Mapping the Chemical Shift Changes. (A) *Spectral Assignment.* $^1H-^{15}N$ -correlated 2D HSQC, ^{15}N -edited 3D TOCSY-HMQC, and ^{15}N -edited 3D NOESY-HMQC spectra, together with $^1H-^1H$ 2D spectra, were used to assign the 1H and ^{15}N backbone resonances of the Fyn SH2 domain (I. D. Campbell, unpublished results). Selective labeling with

$[^{15}N]$ leucine and $[^{15}N]$ glycine samples was also used to assist in and confirm spectral assignment. In general the NMR line widths were relatively broad (corresponding to a correlation time of ~ 10 ns). A few residues (N35, E46, and R73) could not be assigned, and others (H69, K71, T83, and T84) were broad in the presence of peptide. These residues, together with prolines, thus do not appear in the following analysis.

(B) *Binding of the Regulatory Phosphopeptide.* The pY531 tyrosyl 11-residue peptide representing the C-terminal site was added to a 1.5 mM uniformly ^{15}N -labeled SH2 sample in 12 steps, each increasing the peptide concentration by 0.15 mM. A 2D $\{^1H-^{15}N\}$ HSQC experiment was performed after equilibrium had been established on each addition of peptide. Saturation was achieved at a peptide concentration of 1.5 mM. The chemical shift perturbation of many resonances was relatively small. Where changes were observed, most resonances could be traced through the titration.

(C) *Binding of the Specific Peptide.* The 11-residue synthetic phosphopeptide corresponding to the specific SH2-binding site in hmT antigen was added to a 1.5 mM uniformly ^{15}N -labeled SH2 sample in 10 steps, resulting in peptide concentrations of 0.15, 0.3, 0.45, 0.6, 0.75, 0.9, 1.05, 1.2, 1.35, 1.5, and 1.8 mM. Again, a 2D $\{^1H-^{15}N\}$ HSQC experiment was performed at each point of the titration, and saturation was achieved at a 1:1 molar ratio of protein and peptide. The observed chemical shift changes followed the same trend as in the regulatory peptide titration but were generally larger.

(D) *Direct Displacement of the Regulatory Peptide by the Specific Peptide.* Eight aliquots of the specific peptide (to give final concentrations of 0.2, 0.4, 0.6, 0.8, 1.0, 1.2, 1.4, and 1.5 mM) were added to a 1.5 mM sample of ^{15}N -labeled SH2 saturated (2:1) with regulatory peptide, achieving a final ratio of specific peptide to protein to regulatory peptide of 1:1:2. A 2D $\{^1H-^{15}N\}$ HSQC experiment was performed for each point of the titration.

Differential Scanning Calorimetry (DSC). DSC scans of the Fyn SH2 domain were performed to confirm that the polypeptide was in its native state under the experimental conditions adopted in this work. Experiments were done using the MCS DSC (MicroCal Inc., Northampton, MA). A solution of 0.1 mM was placed in the sample cell (volume 1.3 mL) and heated at 1 K/min as described in Ladbury et al. (1992). DSC scans of the SH2 domain under all the conditions used in the experiments reported indicated that the polypeptide was in a fully folded native state and the denaturation curves could be fit to a simple two-state model with both the native and denatured state in a monomeric form.

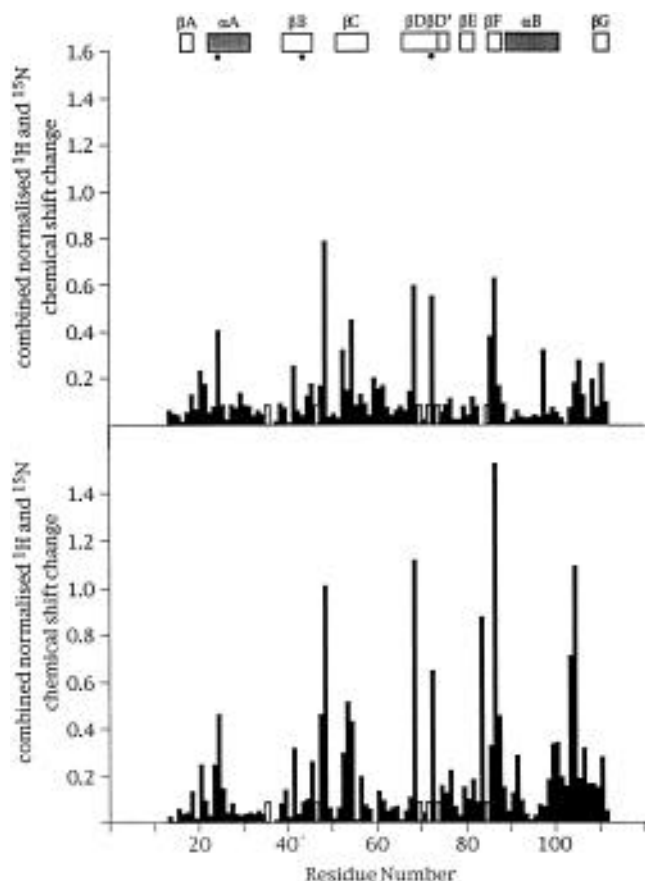


FIGURE 2: Chemical shift changes of amides, in the ^1H and ^{15}N dimensions, observed upon binding saturating amounts of the regulatory (top) and specific (bottom) peptides. Unassigned residues are represented by bars of arbitrary height in the opposite shading. The location of the secondary structural elements is indicated above the plot. Black circles represent residues supposedly involved in anchoring the phosphotyrosine.

RESULTS

NMR Shifts Indicate Two Distinct Modes of Tyrosyl Phosphopeptide Binding. Chemical shift is highly sensitive to changes in the immediate environment of a nuclear spin. It can be used to explore the mode of binding of the two phosphopeptides to the SH2 domain of Fyn. Figure 2 shows the observed chemical shift changes in the ^{15}N and ^1H dimensions for the regulatory, pY531, and the specific, pYHmT, peptides. The total displacement for each residue is expressed as the sum of the normalized changes in the two dimensions. The N-terminal portion of the SH2 domain, which encompasses the pY binding site, shows quite similar chemical shift changes on addition of the two peptides, with both peptides inducing significant chemical shift changes around residue L24 in the AA loop [structural nomenclature of Eck et al. (1993)]. More significant effects are observed around T48 and S53 in the BC loop and in the EF and BG loops. Large changes are also noted on the βD strand (some of these could not be mapped due to line broadening) and the βF strand.

Figure 3 shows the combined $^1\text{H}/^{15}\text{N}$ displacements for each peptide, color coded according to the size of the normalized chemical shift, on a model of the SH2 structure. This clearly shows that the changes observed in the region associated with the pY site are similar on binding of either peptide. However, in the region associated with the pY +

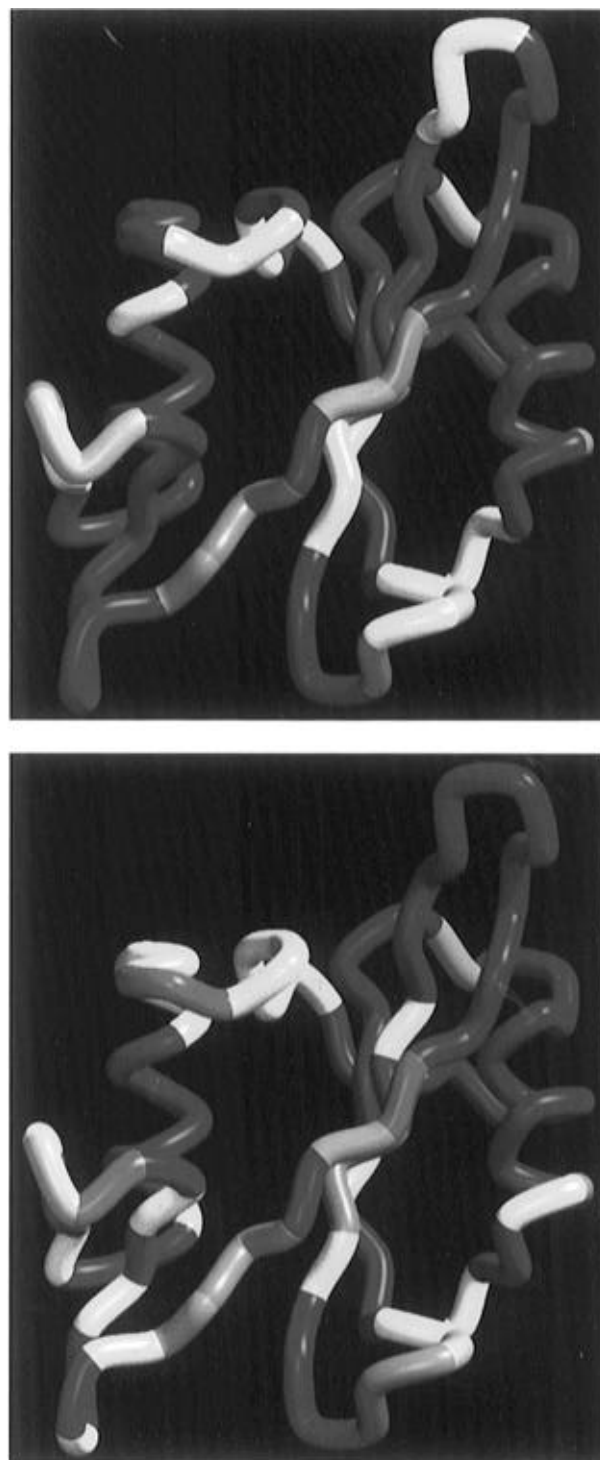


FIGURE 3: Combined ^{15}N – ^1H chemical shift changes on binding, mapped on a backbone representation of the model structure of the Fyn SH2 domain for regulatory (top panel) and specific (bottom panel) peptides. Colors indicate the following ppm ranges: <0.15, blue; 0.15–0.35, yellow; 0.35–0.7, orange; >0.7, red. Gray indicates unassigned residues.

3 residue, the change in chemical shift pattern is significantly different. For the specific peptide (Figure 3, bottom panel) the region encompassed by the EF and BG loops shows large chemical shift changes, suggesting an intimate interaction with the isoleucine residue. This effect is not so pronounced for the regulatory peptide (Figure 3, top panel) where a glycine residue is found in the pY + 3 position. The pY531 peptide makes extensive contact with the loop region between β strands βC and βD . This region is somewhat distal from

the pocket where the pY + 3 residue of the specific peptide binds, suggesting that the regulatory pY531 peptide is not so restricted. This suggests that the pY531 peptide is anchored by its pY residue on the SH2 domain, while residues C-terminal of this can oscillate between other possible positions. The residues in pY + 1 and pY + 2 positions are different for both peptides (EE for pYHmT and QP for pY531). Structural studies on other Src family SH2 domains with bound peptides indicate that these residues lie almost perpendicularly across the β D strand and make contacts through main chain atoms only. Despite the disparate interacting residues this strand exhibits similar contact with either peptide.

Relationship between Thermodynamic and Shift Data. Table 1 shows the thermodynamic parameters for the interaction of the Fyn SH2 domain with both the regulatory and specific peptides obtained by ITC at 25 and 30 °C. The K_D values have been determined using ITC (see Table 1) and by Scatchard analysis of SPR data [at 25 °C and pH 7.4, $K_D(\text{pYHmT}) = 1.09 \mu\text{M}$ and $K_D(\text{pY531}) = 3.38 \mu\text{M}$]. As expected, the specific peptide binds with a higher affinity than the regulatory peptide with a difference of approximately an order of magnitude. The effects of the different buffer conditions under which these measurements were made do not appear to be significant in the case of the specific peptide. These data for the specific peptide interaction are consistent with those previously reported (Ladbury et al., 1995). Data obtained by ITC, for the interaction of the Lck SH2 domain with a peptide corresponding to residues proximal to the regulatory phosphotyrosine, pY505, indicated that at 10 °C the K_D was reduced by approximately an order of magnitude (2.96 to 20.0 μM , respectively; Lemmon & Ladbury, 1994) on going from pH 6.8 to pH 5.5. The data here, obtained at 25 °C, show the same trend on changing the pH from 7.4 to 6.0 (under differing salt conditions) determined by SPR and ITC, respectively. This effect is likely to be due to protonation of the phosphate group since the pK_a of pY is about 5.8 (Domchek et al., 1992). This effect is not observed for the specific peptide and probably arises from the additional interactions made by this peptide with the SH2 domain, with resulting reduction in the pK_a of the bound pY group [see, e.g., Campbell et al. (1979)].

The free energy for the binding interaction, ΔG° , can be deconvoluted into contributions from the ΔH and ΔS° . From Table 1 it can be seen that the enthalpy of interaction for pYHmT is significantly greater than that for the other peptide. This reflects the increased number of hydrogen bonds and van der Waals contacts made by the specific interaction. A large part of this is contributed by the intimate contact of the isoleucine in the SH2 domain pocket which is absent from the pY531 interaction. Comparison of the entropic contribution to ΔG° indicates quite different forms of binding between the two peptides. The ΔS° for the interaction of the SH2 domain with the specific peptide is unfavorable whereas that for the regulatory peptide is favorable. These data are consistent with the observation from NMR spectroscopy that the former is restricted by interaction with the two pockets observed on the surface of the SH2 domain, whereas the latter has more mobility. This would support the hypothesis that pY531 is more dynamic, fluctuating between possible conformations.

Kinetic Analysis of Tyrosyl Phosphopeptide Binding. Observed changes in NMR line shape and intensity on

titration of the pY peptide into the Fyn SH2 domain can provide information on the kinetics of complex formation (Hensmann et al., 1994). Figure 4A,B shows an overlay of the 1D profiles of the peak corresponding to the ^1H resonance of Ala 86. This residue was selected as representative of residues experiencing significant chemical shift changes with either peptide. Several others, however, show similar behavior. The movement of peak positions over the course of the titration clearly reflects two distinct modes of binding for the regulatory and specific peptides. The specific peptide displays characteristic slow-exchange behavior with the peak at the resonance corresponding to the free SH2 domain (P) decreasing in intensity as that for the complex (PL) increases. Neither of the peaks undergoes a chemical shift change. In contrast, binding of the regulatory peptide results in an intermediate exchange pattern. Peak P exhibits strong broadening and change in chemical shift as well as the a reduction in intensity with increasing peptide concentration. At the same time peak PL shows a decrease in line width, significant change in chemical shift, and increase in intensity. Computer simulations representing the closest fit obtained for the experimental data based on one-step and two-step binding models are shown in Figure 4C,D. The specific peptide is best fit by simple exchange between P and PL states—the change in ligand concentration is simulated by incrementing the on rate while the off rate is set to remain at $12 \pm 2 \text{ s}^{-1}$. Titration of the regulatory peptide cannot be simulated by simple exchange between P and PL states. The fit shown was obtained by employing an overall off rate of 100 s^{-1} in a three-site model (P, PL, and P*L, where P*L corresponds to some additional bound state). The chemical shift displacement of the peak corresponding to PL could not be reproduced in any of the many simulations attempted. The kinetic mechanism of complex formation with the regulatory peptide must therefore involve either more than two steps or several distinct binding modes with different chemical shifts in the various PL states.

SPR kinetic analysis employing curve fitting of sensorgrams yielded off rates for the SH2 interactions of the specific and regulatory peptides. Off-rate values of approximately 0.2 and 1 s^{-1} were obtained for the specific and regulatory peptides, respectively. The on rates in both cases were of the order $2 \times 10^5 \text{ M}^{-1} \text{ s}^{-1}$. The off rates determined by SPR are significantly different from those derived from the NMR analysis, as previously observed for the p85 SH2 domain—tyrosyl phosphopeptide interaction (Hensmann et al., 1994). The differences may be partly explained by the fact that the data were, for essential practical reasons, obtained under somewhat different conditions (see Experimental Procedures). It also worth noting that, in NMR, the sample is a concentrated solution of the SH2 domain and peptide at equilibrium, while SPR, which involves covalent linkage of one of the interacting components to a Dextran matrix and the flow of the other component, occurs in a very different environment to NMR and is prone to artifacts [see Ladbury et al. (1995)].

Displacement of the Regulatory Peptide by the Specific Peptide. Figure 5 shows a sequence of eight $\{^1\text{H}-^{15}\text{N}\}$ HSQC spectra on addition of aliquots of a specific peptide to a sample of the Fyn SH2 domain with the pY531 peptide. The final concentration ratio is 1:1:2 for the SH2 domain, pYHmT, and pY531, respectively. The spectra highlight the change in chemical shift of Ala 86 which, as described above,

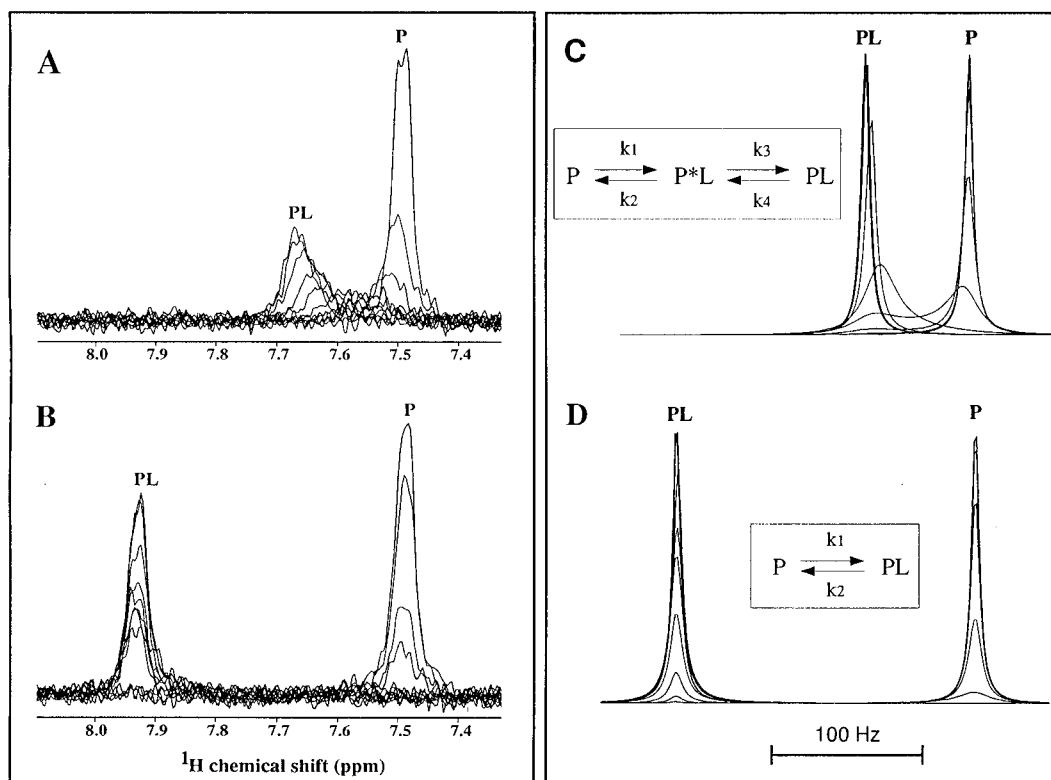


FIGURE 4: Superposition of ^1H cross sections of 2D experiments for Ala 86 in the Fyn SH2 domain, obtained in a titration of (A) the regulatory peptide and (B) the specific peptide. P and PL indicate the positions of the resonances in the free and peptide-bound states, respectively. The observed behavior is representative of several significantly shifted residues in the protein. (C) and (D) show line-shape simulations of the experimental data in (A) and (B). The exchange model used is shown boxed. (D) corresponds to a simple two-site chemical exchange model with peak separation set to 200 Hz, line width to 8 Hz, and off rate to 10 s^{-1} ; (C) is simulated by a linear three-site exchange model with PL/P peak separation set to 70 Hz.

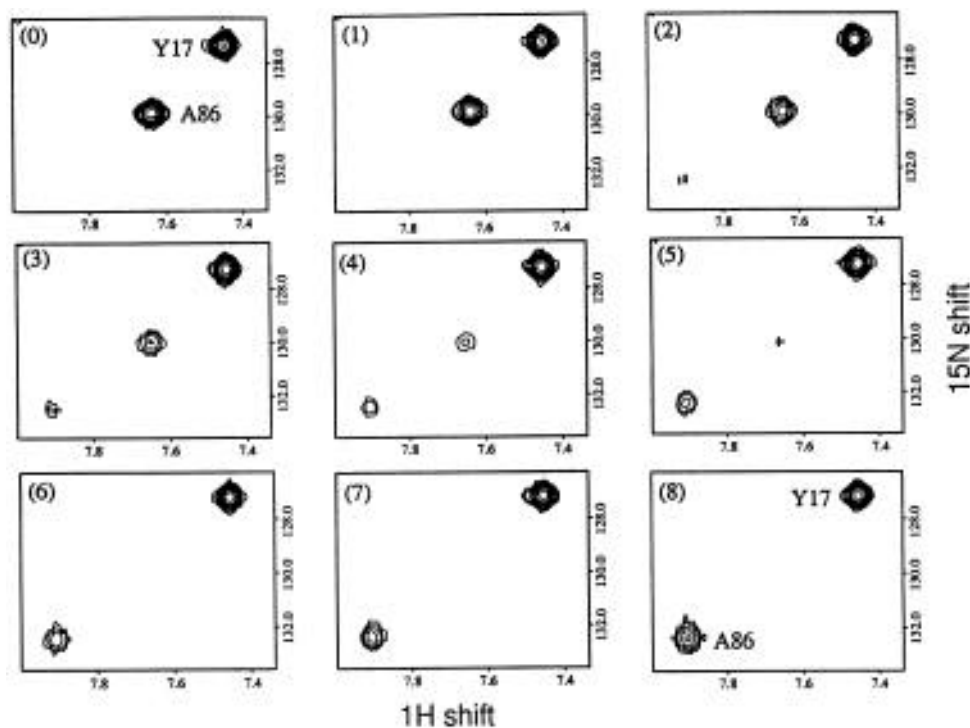


FIGURE 5: $\{^1\text{H}-^{15}\text{N}\}$ HSQC spectrum of the Fyn SH2 domain showing the displacement of the peak corresponding to Ala 86 when specific peptide is titrated into a sample of the protein saturated with regulatory peptide. See Experimental Procedures for concentrations of peptides and SH2 domain for each aliquot.

is typical of resonances perturbed by peptide binding. As the concentration of the specific peptide is increased, the chemical shift of the peak assigned to A86 is shifted to the

position where it is seen in the pYHmT-SH2 domain complex. These data confirm that the regulatory peptide is displaced by the specific peptide in solution.

DISCUSSION

Knowledge of regulatory mechanisms of key enzymes is crucial to an understanding of signal transduction as a whole. Here we have addressed this issue by studying the structural, thermodynamic, and kinetic effect on binding two different tyrosyl phosphopeptides to a Src family SH2 domain—one from the C-terminal regulatory region and the other from a putative specific natural ligand. The correlation of data obtained from three complementary techniques enables a detailed picture of the binding mechanism to be established.

The NMR shift data indicate that the interaction of both peptides involves the insertion of the pY side chain into a pocket. This is the pivotal interaction and appears to contribute a significant part of the total free energy of formation of the complex. This is consistent with structural studies of SH2–pY-peptide complexes that showed a network of hydrogen bonds between the phosphotyrosine and the SH2 domain (Eck et al., 1993; Waksman et al., 1993; Lee et al., 1994; Hatada, 1995). The regions of the peptides C-terminal to the pY groups, however, bind quite differently.

In the interaction with the specific pYHmT peptide, the isoleucine in the pY + 3 position of the peptide also appears to insert into a defined pocket as shown by both the NMR shift data (Figure 3) and the line-shape analysis (Figure 4). The isoleucine side chain in this position is in contact with a number of hydrophobic residues, and the resulting van der Waals interactions improve the free energy of binding for the “two-pronged plug” complex. This is reflected in the negative enthalpy of binding. Polypeptide interactions incur an entropic penalty by restricting side chain vibrational modes compared to the unbound state; this is likely to be the cause of the observed unfavorable ΔS° for the interaction of the SH2 domain with the specific peptide (Table 1).

While the specific ligand makes intimate contact with both the pY and the pY + 3 pockets, the regulatory peptide only inserts in a defined way into the pY pocket, with the C-terminal region fluctuating between other possible positions. This concept is consistent with both the shift data (Figure 3) and the line-shape analysis (Figure 4). The ΔS° for the interaction of the SH2 domain with this peptide is favorable (Table 1), corroborating the conclusion that the regulatory peptide is not attached throughout its length but has more degrees of freedom. Furthermore, the specific peptide has a larger enthalpic contribution, suggesting the formation of a larger number of noncovalent bonds. It should be noted that other effects could play a role; for example, the respective degrees of freedom on going from the free to the bound state and the solvent interactions will be different for each peptide because of differences in residues.

Recent studies on the dynamics of the interaction of a pY peptide corresponding to a region of the high-affinity binding site on β -platelet-derived growth factor receptor with the C-terminal SH2 domain from PLC- γ give detailed information about the involvement of individual residues in binding (Farrow et al., 1994; Pascal et al., 1995; Kay et al., 1996). In one case, the differential order parameters of methyl groups on SH2 domain amino acid side chains in the pY insertion pocket were reduced on going from free to complexed states; this was interpreted as the pY side chain insertion leading to a tightening of structure in the pocket (Kay et al., 1996). Dynamic studies of the interaction of the proline residue in the pY + 3 position of the peptide

with the hydrophobic pocket of the SH2 domain indicated that residues in this region have a high degree of mobility in both the free and complexed states (Kay et al., 1996). It would be interesting to see if the observations could be resolved thermodynamically as we have done here.

It is of interest to consider the current models for Src tyrosine kinase regulation in light of our studies. These involve the C-terminal pY playing an autoregulatory role by back-binding either to the intramolecular SH2 domain or with another similar protein in a head-to-tail dimer. The binding of regulatory peptide has been shown here to be weaker than that of the specific interaction, but for the intramolecular interaction, the effective local concentrations of this binding region will be relatively high. For example, it was found that millimolar concentrations of free S-peptide, which binds to ribonuclease S with a K_D in the micromolar range, were required to give the same stability as the wild-type ribonuclease A (where the S-peptide forms the N-terminus of the protein; Labhardt, 1981). SH2 domain autoregulation has also recently been reported for the Crk adaptor protein (Rosen et al., 1995). In the case of regulation by a head-to-tail homodimer where two pY peptide–SH2 domain interactions occur, any competition for the SH2 site from a potential ligand is likely to disrupt both pY–SH2 interactions. The total free energy to prize apart the two interlocking molecules would be significant, and regulation by this mechanism would require a tight binding or large concentrations of a potential interacting ligand.

To what extent pY peptides binding to isolated SH2 domains represent *in vivo* protein–protein interactions is an interesting question. It is likely that the binding of a linear peptide lacks some of the contacts that will be made on presenting the three-dimensional surface of an intact protein. Furthermore, the peptide is unlikely to be presented in the form adopted in solution when it is within the secondary structural context of an intact protein. However, various structural studies of peptide–SH2 interactions have provided some insight into the specificity of SH2-mediated interactions and defined interactions that are crucial in recognition which are likely to be equally important in protein–protein interactions. Information on the binding of peptides with SH2 domains can provide valuable insight to approaches for pharmaceutical intervention since key interactions are identified and, thus, can be targeted by potential drug compounds.

From the data presented here it is clear that the mechanisms for interaction of a specific versus a regulatory peptide are distinctly different from structural, thermodynamic, and kinetic standpoints. The additional specificity imposed by regulation in Src family kinases appears to be based on competition for a binding site where the weaker interaction made by dynamic residues C-terminal of pY leaves the hydrophobic pocket for binding the pY + 3 residue partially occupied. The specific interaction involves intimate contact with this pocket which is sufficient to overcome this weaker interaction by insertion of a side chain into the hydrophobic pocket.

ACKNOWLEDGMENT

We thank colleagues Alessandro Pintar and Craig Morton for assistance with NMR studies of the SH2 domain, Jonathan Boyd for writing computer programs for line-shape analysis, and Maureen Pitkeathly for preparation of peptides.

REFERENCES

- Campbell, I. D., Jones, R. B., Kiener, P. A., Waley, S. G. (1979) *Biochem. J.* 179, 607–621.
- Cantley, L. C., Auger, K. R., Carpenter, C., Duckworth, B., Graziani, A., Kapeller, R., & Soltoff, S. (1991) *Cell* 64, 281–302.
- Cooper, J. A., & Rothwell, B. (1993) *Cell* 73, 1051–1054.
- Courtneidge, S. A., Groutebroze, L., Cartwright, A., Heber, A., Scherneck, S., & Feunteun, J. (1991) *J. Virol.* 65, 3301–3308.
- Eck, M. J., Shoelson, S. E., & Harrison, S. C. (1993) *Nature* 362, 87–91.
- Eck, M. J., Atwell, S. K., Shoelson, S. E., & Harrison, S. C. (1994) *Nature* 368, 764–769.
- Domchek, S., Auger, K., Chatterjee, S., Burke, T., Jr., & Shoelson, S. E. (1992) *Biochemistry* 31, 9865–9870.
- Farrow, N. A., Muhandiram, R., Singer, A. U., Pascal, S. M., Kay, C. M., Gish, G., Shoelson, S. E., Pawson, T., Forman-Kay, J. D., & Kay, L. E. (1994) *Biochemistry* 33, 5984–6003.
- Hatada, M. H., Lu, X., Laird, E. R., Green, J., Morgenstern, J. P., Lou, M., Marr, C. S., Phillips, T. B., Ram, M. K., Thierault, K., Zoller, M. J., & Karas, J. L. (1995) *Nature* 377, 32–38.
- Hensmann, M., Booker, G. W., Panayotou, G., Boyd, J., Linacre, J., Waterfield, M., & Campbell, I. D. (1994) *Protein Sci.* 3, 1020–1030.
- Kay, L. E., Muhandiram, D. R., Farrow, N. A., Aubin, Y., & Forman-Kay, J. D. (1996) *Biochemistry* 35, 361–368.
- Kitas, E. A., Knorr, R., Trzeciak, A., & Bannwarth, W. (1993) *Helv. Chim. Acta* 74, 1314–1328.
- Kuriyan, J., & Cowburn, D. (1993) *Curr. Opin. Struct. Biol.* 3, 828–837.
- Labhardt, A. M. (1981) *Biopolymers* 20, 1459–1480.
- Ladbury, J. E., Hu, C.-Q., & Sturtevant, J. M. (1992) *Biochemistry* 31, 10699–10702.
- Ladbury, J. E., Lemmon, M. A., Zhou, M., Green, J., Botfield, M. C., & Schlessinger, J. (1995) *Proc. Natl. Acad. Sci. U.S.A.* 92, 3199–3203.
- Lee, C.-H., Kominos, D., Jacques, S., Margolis, B., Schlessinger, J., Shoelson, S. E., & Kuriyan, J. (1994) *Structure* 2, 423–438.
- Lemmon, M. A., & Ladbury, J. E. (1994) *Biochemistry* 33, 5070–5076.
- Marion, D., Ikura, M., Tschudin, R., & Bax, A. (1989) *J. Magn. Reson.* 85, 393–399.
- Mikol, V., Baumann, G., Keller, T. H., Manning, U., & Zurini, M. G. M. (1995) *J. Mol. Biol.* 246, 344–355.
- Panayotou, G., Gish, G., End, P., Truong, O., Gout, I., Dhand, R., Fry, M. J., Hile, I., Pawson, T., & Waterfield, M. D. (1993) *Mol. Cell. Biol.* 13, 3567–3576.
- Pascal, S. M., Yamazaki, T., Singer, A. U., Kay, L. E., & Forman-Kay, J. D. (1995) *Biochemistry* 34, 11353–11362.
- Pawson, T. (1994) *Nature* 373, 573–580.
- Pawson, T., & Schlessinger, J. (1993) *Curr. Biol.* 3, 434–442.
- Payne, G., Shoelson, S. E., Gish, G., Pawson, T., & Walsh, C. T. (1993) *Proc. Natl. Acad. Sci. U.S.A.* 90, 4902–4906.
- Piccione, E., Case, R. D., Domchek, S. M., Hu, P., Chaudhuri, M., Backer, J. M., Schlessinger, J., & Shoelson, S. E. (1993) *Biochemistry* 32, 3197–3201.
- Rosen, M. K., Yamazaki, T., Gish, G. D., Kay, C. M., Pawson, T., & Kay, L. E. (1995) *Nature* 374, 477–478.
- Schlessinger, J. (1994) *Curr. Opin. Genet. Dev.* 4, 25–30.
- Semba, K., Nishizawa, M., Miyajima, N., Yoshida, M. C., Sukegawa, J., Yamanishi, Y., Sasaki, M., Yamamoto, T., & Toyoshima, K. (1986) *Proc. Natl. Acad. Sci. U.S.A.* 83, 5459–5463.
- Shaka, A. J., Barker, P. B., & Freeman, R. (1985) *J. Magn. Reson.* 64, 547–552.
- Songyang, Z., & Cantley, L. C. (1995) *Trends Biochem. Sci.* 20, 470–475.
- Songyang, Z., Shoelson, S. E., Chaudhuri, M., Gish, G., Pawson, T., Haser, W. G., King, F., Roberts, T., Ratnofsky, S., Lechleider, R. J., Neel, B. G., Birge, R. B., Fujardo, J. E., Chou, M. M., Hanafusa, H., Schaffhausen, B., & Cantley, L. C. (1993) *Cell* 72, 767–778.
- Waksman, G., Kominos, D., Robertson, S. C., Pant, N., Baltimore, D., Birge, R. B., Cowburn, D., Hanafusa, H., Mayer, B. J., Overduin, M., Resh, M. D., Rios, C. B., Silverman, L., & Kuriyan, J. (1992) *Nature* 359, 646–653.
- Waksman, G., Shoelson, S. E., Pant, N., Cowburn, D., & Kuriyan, J. (1993) *Cell* 72, 779–790.
- Wiseman, T., Williston, S., Brandts, J. F., & Lin, L.-N. (1989) *Anal. Biochem.* 179, 131–137.

BI960543E